Composite wing elastic axis for aeroelasticity optimization design

S.H. Huo, F.S. Wang, Z. Yuan and Z.F. Yue
Advanced Materials Test Center, School of Mechanics Civil Engineering and Architecture, Northwestern Polytechnical University, Xi'an, People's Republic of China

Abstract

Purpose – Computational efficiency is always the major concern in aircraft design. The purpose of this paper is to investigate an efficient aeroelasticity optimization design method. Analysis of composite wing elastic axis is presented in the current study and its application on aeroelasticity optimization design is discussed.

Design/methodology/approach – Elastic axis consists of stiffness centers. The stiffness centers of eight cross sections are analyzed and the wing elastic axis is obtained through least-squares procedure. In the analysis of the cross section stiffness center, the wing model is approximated by assuming the wing cross section as a thin walled structure with a single cell closed section and assuming the composite material to be a 3D anisotropic material. In aeroelasticity optimization design, objective functions are taken to be the wing weight and elastic axis position. Design variables are the thickness and area of wing components.

Findings – After aeroelasticity optimization design, the wing weight decreases while the divergent velocity increases. Meanwhile, it can achieve an expected result but costs much less computational time than the conventional method.

Practical implications – The results can be used for aircraft design or as an initial value for the next detailed optimization design.

Originality/value – The computational time can be dramatically reduced through the aeroelasticity optimization design based on the elastic axis. It is suitable for engineering applications.

Keywords Air transport engineering, Design, Composite wing, Elastic axis, Divergent velocity, Aeroelasticity optimization design, Multi-Island genetic algorithm

Paper type Research paper

Introduction

Aeroelasticity is always the major concern in aircraft design. Aircraft structure is elastic. Elastic deformation, which is the result of initial aerodynamic function, will lead to additional aerodynamic load. Additional aerodynamic load will lead to a new elastic deformation. Aircraft structure will obtain a balanced state or deform gradually until structural damage happens. There is a critical speed for each specified aircraft, which is defined as divergent velocity. Both aircraft layout and mass distribution have a direct impact on the divergent velocity. Higher divergent velocity and lighter weight of the aircraft are the targets of aircraft design. The optimization design, especially multi-disciplinary design optimization (MDO), is widely used in aircraft design.

Aeroelasticity optimization design which considers both weight and aerodynamic characteristic is a branch of MDO. Many scholars dedicated to research in this field and a lot of methods were put forward. Wakayama (2000) showed an initial structural optimization which has not a proper MDO framework. As the development of computational fluid dynamic (CFD) models, Guruswamy and Obayashi (2004) and Yang *et al.* (2005) developed a particularly true MDO framework for the aerodynamic shape optimization. Unfortunately, the computational time of MDO analysis increased drastically. For reducing the time, Zhang *et al.* (2008) proposed surrogate models. At the same time, many algorithmic methods which reproduce some natural phenomena or physical processes were proposed, such as Genetic and Evolutionary Algorithms (Alonso *et al.*, 2009), Swarm Intelligence (Venter and Sobieszczanski-Sobieski, 2004) and Simulated Annealing (Jeon *et al.*, 2008).

In aeroelasticity optimization design, the objective function correlates closely with the divergence speed and structure mass. Guo *et al.* (2003) demonstrated that a significant increase of flutter speed can be achieved by optimizing the wing skin thickness or the laminate layups. Kameyama and Fukunaga (2007) investigated the effect of laminate configuration on the aeroelasticity characteristics and optimization design of composite plate wings using lamination parameters. Barcelos and Maute (2008) studied a general optimization methodology for fluid-structure interaction problems based on turbulent flow models. Librescu and Maalawi (2009) presented the aeroelasticity optimization of a wing-type structure through a novel mathematical approach. Mastroddi *et al.* (2011) studied the initial design of wing structures based on the integrated modeling of structures, aerodynamic, flight dynamics and aeroelasticity. Chintapalli *et al.* (2010) investigated a layout

The current issue and full text archive of this journal is available at **www.emeraldinsight.com/1748-8842.htm**

Aircraft Engineering and Aerospace Technology: An International Journal
85/1 (2013) 10–15
 [ISSN 1748-8842]
[DOI 10.1108/00022661311294030]

This study is supported by the National Natural Science Foundation of China (No. 50905142) and Shaanxi Provincial Natural Science Foundation (No. 2009JQ1006).

Aircraft Engineering and Aerospace Technology: An International Journal
Volume 85 · Number 1 · 2013 · 10–15

optimization method of a skin-stringer panel for an aircraft wing-box. They all investigated the accuracy and efficiency of aircraft aeroelasticity optimization design and some considerable methods were proposed. However, computational efficiency still has an obvious impact on aircraft design, but it is not often addressed.

Stiffness characteristic has an impact on aeroelasticity. Serious aeroelasticity problems may occur under an irrational stiffness characteristic design. Elastic axis plays an important role in stiffness characteristic. The present work aims at investigating the composite wing elastic axis and its application on the aeroelasticity optimization design.

Analysis of composite wing elastic axis

Stiffness characteristic of the wing structure has a high correlation with the location of elastic axis. Hence, an appropriate location of the elastic axis is important in engineering design. Here, the location of elastic axis analysis is carried out on a composite wing structure.

Composite wing configuration

The composite wing shown in Figure 1 is composed of skin, spar, rib and stringer. It is a primal finite element model. NACA0012 airfoil is adopted in the model. The chord length of the wing root is 2,500 mm while the wing tip is 1,500 mm. The span which has a back swept angle of 20° is 16,000 mm. The material of all components is T300/QY8911. Its material properties are shown in Table I. Table II shows the specific laminate layup and thickness of every component. The length and thickness of spar flange is 100 mm and 6 mm, respectively. The thickness of spar web is 5 mm. For T shaped stringer, the length and thickness of flange are 60 mm and 4 mm, respectively, and those of web are 80 mm and 4.8 mm.

Figure 1 Finite element model of composite wing

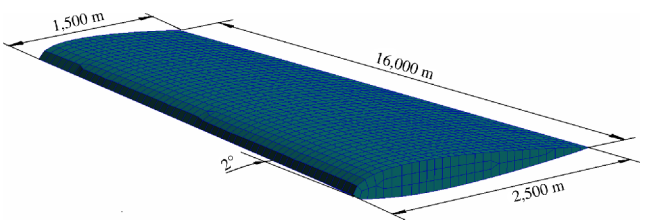

Table I Material property of T300/QY8911

E_{11}/MPa	E_{22}/MPa	E_{33}/MPa	G_{12}/MPa	G_{23}/MPa	G_{13}/MPa	ν_{12}	ν_{23}	ν_{13}
135,000	8,800	8,800	4,470	3,200	4,470	0.33	0.48	0.15

Table II Laminate layup of every component

Component	Layup	Thickness (mm)
Skin	$[0/90/0/45/-45/0/90/0/45/-45]_S$	4
Spar	$[0/45/-45/90/0/45/-45/0/45/-45]_S$	–
Rib	$[0/90/0/45/-45/0/90/0/45/-45]_S$	4
Stringer	$[0/45/-45/0/90/0/90/0/-45/45]_S$	–

Simplified model

Elastic axis is a position where only bending happens when the load is applied on it. Elastic axis is composed of many wing cross section stiffness centers. The wing cross section is simplified to a thin walled structure with a single cell closed section. In the two dimensional cross section model, skin and spar web are simplified as some lines while stringer and spar flange are simplified as some points. Two equivalent processes, area equivalent and material equivalent, are carried out for the model simplifying.

(1) Area equivalent

Cross section area of each component has a direct effect on stiffness center. For skin, all of the cross section areas are effective. For part of skin which locates within the interval of [a, b], its effective area can be written as:

$$A_{skin} = \int_a^b tds \tag{1}$$

where A_{skin} is skin effective area and t is skin thickness.

For stringer, it has been simplified to an intensive area above which is shown as a dot. Usually, the dot needs to be lain in the line obtained from the simplified skin. So the stringer area needs to be reduced, it can be written as:

$$A^*_{stringer} = A_{stringer}\frac{h_1^2}{h_0^2} \tag{2}$$

where $A^*_{stringer}$ and $A_{stringer}$ are the reduced and initial area, respectively, h_1 is the distance from the skin to the neutral surface of airfoil cross section, and h_0 is the distance from the stringer centroid to the neutral surface of the airfoil cross section.

For the spar, top and down flanges are reduced to an intensive area just as the method in stringer treatment while the web is treated in the same way as used for the skin.

(2) Material equivalent

Skin, stringer and spar have their own different layups, so it is necessary to select one of them as material sample and others equivalent to it. A reduction factor φ is introduced and written as:

$$\varphi = \frac{E_i}{E_0} \tag{3}$$

where E_i is Young's modulus of practical material and E_0 is that of material sample.

In the present study, composite material is converted into a 3D anisotropic material based on the stiffness matrix (Dong *et al.*, 2010). For an orthotropic laminate, the stress-strain relationship of each layup under 3D stress condition can be written as:

$$\begin{Bmatrix}\sigma_x\\ \sigma_y\\ \sigma_z\\ \tau_{yz}\\ \tau_{zx}\\ \tau_{xy}\end{Bmatrix} = \begin{bmatrix} Q_{11} & Q_{12} & Q_{13} & & & \\ Q_{21} & Q_{22} & Q_{23} & & & \\ Q_{31} & Q_{32} & Q_{33} & & & \\ & & & Q_{44} & & \\ & & & & Q_{55} & \\ & & & & & Q_{66}\end{bmatrix}\begin{Bmatrix}\varepsilon_x\\ \varepsilon_y\\ \varepsilon_z\\ \gamma_{yz}\\ \gamma_{zx}\\ \gamma_{xy}\end{Bmatrix} \tag{4}$$

Because the principle axis of each layup may not coincident with the global coordinate axis, the material stiffness matrix with

respect to the material coordinate system needs to be converted into that under the global coordinate system. Introducing the stress transfer matrix $[T]$ and the router matrix $[R]$, the stress-strain relationship can be rewritten as:

$$\begin{Bmatrix} \sigma_x \\ \sigma_y \\ \sigma_z \\ \tau_{yz} \\ \tau_{zx} \\ \tau_{xy} \end{Bmatrix} = [T]^{-1} \begin{Bmatrix} \sigma_1 \\ \sigma_2 \\ \sigma_3 \\ \tau_{23} \\ \tau_{13} \\ \tau_{12} \end{Bmatrix} = [T]^{-1}[Q] \begin{Bmatrix} \varepsilon_1 \\ \varepsilon_2 \\ \varepsilon_3 \\ \gamma_{23} \\ \gamma_{13} \\ \gamma_{12} \end{Bmatrix} = [T]^{-1}[Q][R][T][R]^{-1} \begin{Bmatrix} \varepsilon_x \\ \varepsilon_y \\ \varepsilon_z \\ \gamma_{yz} \\ \gamma_{zx} \\ \gamma_{xy} \end{Bmatrix} \tag{5}$$

Therefore, stiffness matrix under partial coordinate system can be written as:

$$[Q]^{-1} = [T]^{-1}[Q][R][T][R]^{-1} \tag{6}$$

Based on equation (6), the stiffness matrix of each layup under the global coordinate system can be written as:

$$[\overline{Q_{ij}}]_k = \begin{bmatrix} \overline{Q_{11}} & \overline{Q_{12}} & \overline{Q_{13}} & 0 & 0 & \overline{Q_{16}} \\ \overline{Q_{12}} & \overline{Q_{22}} & \overline{Q_{23}} & 0 & 0 & \overline{Q_{26}} \\ \overline{Q_{13}} & \overline{Q_{23}} & \overline{Q_{33}} & 0 & 0 & \overline{Q_{36}} \\ 0 & 0 & 0 & \overline{Q_{44}} & \overline{Q_{45}} & 0 \\ 0 & 0 & 0 & \overline{Q_{45}} & \overline{Q_{55}} & 0 \\ \overline{Q_{16}} & \overline{Q_{26}} & \overline{Q_{36}} & 0 & 0 & \overline{Q_{66}} \end{bmatrix} \tag{7}$$

The laminate equivalent stiffness matrix can be written as:

$$[\overline{Q_{ij}}] = \frac{\sum_{k=1}^{N} [\overline{Q_{ij}}]_k d_k}{t} \tag{8}$$

where N is the number of layup, d_k is the thickness of the kth layer and t is the thickness of laminate. For a skew-symetric laminate, $\overline{Q_{16}} = \overline{Q_{26}} = \overline{Q_{36}} = \overline{Q_{45}} = 0$ because they are odd functions of the layup angle. Then, the stiffen matrix can be written as:

$$[\overline{Q_{ij}}] = \begin{bmatrix} \overline{Q_{11}} & \overline{Q_{12}} & \overline{Q_{13}} & 0 & 0 & 0 \\ \overline{Q_{12}} & \overline{Q_{22}} & \overline{Q_{23}} & 0 & 0 & 0 \\ \overline{Q_{13}} & \overline{Q_{23}} & \overline{Q_{33}} & 0 & 0 & 0 \\ 0 & 0 & 0 & \overline{Q_{44}} & 0 & 0 \\ 0 & 0 & 0 & 0 & \overline{Q_{55}} & 0 \\ 0 & 0 & 0 & 0 & 0 & \overline{Q_{66}} \end{bmatrix} \tag{9}$$

Hence, the composite material has been converted into 3D anisotropic material and its Young's modulus can be obtained from the material stiffen matrix.

Position of elastic axis

One of the wing cross sections is selected for introducing the stiffness center computation method (Liu *et al.*, 2006). The wing cross section is composed of ten stringers, four spar flanges, two spar webs and skin among two intensive area positions. Table III shows the area and coordinate of the initial wing intensive area. In Table III, B_i and S_i are the intensive area of spar flange and stringer, respectively.

The area of each wing cross section component and the area centroid can be obtained through:

$$\begin{aligned} A &= \oint \varphi_i t_i ds + \sum_i \varphi_i A_i \\ \xi_0 &= \frac{\oint \varphi_i t_i x_i ds + \sum_i \varphi_i A_i x_i}{A} \\ \eta_0 &= \frac{\oint \varphi_i t_i y_i ds + \sum_i \varphi_i A_i y_i}{A} \end{aligned} \tag{10}$$

Where φ_i is the reduction factor, t_i is the thickness of skin, A is the total area of all component cross section, and ξ_0 and η_0 are x and y coordinate value of centroid, respectively.

Because the computation of stiffness center will be carried out in inertia axis, it is necessary to transfer the coordinate, which can be done by subtracting the value of centroid. Then, the area moment of inertia of the reduced cross section with respect to the inertia axis can be obtained as:

$$\begin{aligned} \mathcal{J}_x &= \oint y_i^2 \varphi_i t_i ds + \sum_i \varphi_i A_i y_i^2 \\ \mathcal{J}_y &= \oint x_i^2 \varphi_i t_i ds + \sum_i \varphi_i A_i x_i^2 \end{aligned} \tag{11}$$

The moment of the area of reduced cross section with respect to the inertia axis can be obtained as:

$$\begin{aligned} S_x &= \oint y_i \varphi_i t_i ds + \sum_i \varphi_i A_i y_i \\ S_y &= \oint x_i \varphi_i t_i ds + \sum_i \varphi_i A_i x_i \end{aligned} \tag{12}$$

Based on the structural mechanics theory, the stiffness center of a cross section can be obtained as:

$$\begin{aligned} X &= \frac{1}{\mathcal{J}_x} \left(\int_s S_x \rho ds - \Omega \frac{\oint (S_x/Gt) ds}{\oint (ds/Gt)} \right) \\ Y &= \frac{1}{\mathcal{J}_y} \left(\int_s S_y \rho ds - \Omega \frac{\oint (S_y/Gt) ds}{\oint (ds/Gt)} \right) \end{aligned} \tag{13}$$

where ρ is the distance from the area centroid to the tangent of each component, and Ω is two times the enclosed cross section.

Through the method above, it can be obtained that the distance from the stiffness center to the leading edge is 44.41 percent of the chord length.

Eight wing cross sections are selected and their stiffness centers are obtained. Then the wing elastic axis position can be obtained through least-squares procedure.

Effects of elastic axis on aeroelasticity

Take a two dimensional wing for example, bending and torsion of the wing were simulated as sink-float and pitch of the airfoil

Table III Area and coordinate of the initial wing intensive area

Top skin				Down skin			
Serial number	x/mm	y/mm	Area/mm^2	Serial number	x/mm	y/mm	Area/mm^2
B_1	2,394.48	139.08	600	B_3	2,392.18	−69.54	600
B_2	3,505.33	70.53	600	B_4	3,502.67	−49.53	600
S_1	2,556.49	144.34	624	S_6	2,551.51	−81.38	624
S_2	2,737.94	140.64	624	S_7	2,732.94	−85.69	624
S_3	2,932.04	129.41	624	S_8	2,927.35	−83.05	624
S_4	3,130.37	112.56	624	S_9	3,126.22	−74.96	624
S_5	3,324.28	92.23	624	S_{10}	3,320.84	−63.21	624

(Palacios and Cesnik, 2005). Because aerodynamic load caused by sink-float is feeble, only pitch is considered in airfoil aeroelasticity problems. Practical airfoil attack angle α is composed of initial attack angle α_0 and torsion angle θ under the function of aerodynamic. Moment of aerodynamic on the stiffness center, M_e, can be written as:

$$M_e = q_d S c C_{MAC} + q_d S \left[\frac{\partial C_L}{\partial \alpha}(\alpha_0 + \theta)\right] e \tag{14}$$

where q_d is the dynamic pressure, S is the airfoil area, c is the cross section chord length, C_{MAC} is the moment coefficient, $(\partial C_L)/(\partial \alpha)$ is the slope of lift curve and e is the distance from the stiffness center to the aerodynamic center.

Two springs are adopted to simulate constraints of the airfoil. Equilibrium equation of aerodynamic moment and spring elastic moment is written as:

$$q_d S \left[\frac{\partial C_L}{\partial \alpha}(\alpha_0 + \theta)\right] e + q_d c S C_{MAC} = k_\alpha \theta \tag{15}$$

where k_α is the spring elastic coefficient. So the torsion angle θ can be obtained and written as:

$$\theta = \frac{(q_d S)/(k_\alpha)(e(\partial C_L/\partial \alpha)\alpha_0 + cC_{MAC})}{1 - ((q_d e S)/k_\alpha)(\partial C_L/\partial \alpha)} \tag{16}$$

The torsion angle becomes infinite when the denominator of equation (16) equals to zero, indicating that the wing is in a divergent state. Hence, the divergent velocity, V_D, can be written as:

$$V_D = \sqrt{\frac{2k_\alpha}{\rho_\alpha e S \partial C_L/\partial \alpha}} \tag{17}$$

From equation (17), it can be seen that divergent velocity decreases with the increase of e. Hence, the location of the stiffness center has a direct impact on the wing divergent velocity. A stiffness center closer to the aerodynamic center by changing the wing layout is preferred in wing design.

Optimization design based on elastic axis

For general multi-disciplinary optimization problems, it can be described by an optimum objective function $F(f(x_1), f(x_2), \ldots, f(x_n))$, constraint condition $(g_j(X) < 0 \ (j = 1, 2, \ldots, m))$ or $h_j(X) = 0 \ (j = m+1, \ldots, n)$ and design variables $X_L \le X \le X_U$, $X = (X_1, X_2, \ldots, X_n)^T$ (Riche and Haftka, 1993).

Optimization parameters

Wing weight and the distance from the stiffness center to the leading edge point are two objective functions in the present study. The optimum objective function can be written as:

$$F = \frac{W_1 G}{G_m} + \frac{W_2 e}{l} \tag{18}$$

where G is the wing weight after optimization, G_m is the maximum wing weight in design variable span, e is the distance from the stiffness center to the leading edge, l is the cross section chord, and W_1 and W_2 are weight coefficients.

Constraint conditions are selected based on structural characteristics. The maximum torsion angle, maximum elastic axis flexivity and stability are constraint conditions. Table IV shows their specific values.

The stress is not uniformly distributed over the wing. So, different region thickness values advantage wing design. Figure 2 shows the regions divided in the composite wing. As shown in Figure 2, the finite element model of the wing structure is divided into 20 regions. In each region, skins, spars, ribs and stringers have their own independent design variables. Thickness is the most important design variable in the present work.

Optimization process

Whole optimization process is carried out using the software iSIGHT. Multi-island genetic algorithm is used for wing optimization design. Static strength and stability are analyzed after setting initial model design parameters. It can be judged from the result that whether the model meets constraint conditions. If it does, the wing weight and the position of elastic axis are output. If not, design parameters need to be modified and computed again. Static strength and stability are analyzed through FEM software NASTRAN while the position of elastic axis in the FORTRAN code is based on the introduction above. Figure 3 shows the optimization process. As shown in Figure 3, the stop condition can be expressed as:

Table IV Values of constraint conditions

Constraint condition	Value
Maximum tensile strain	$\lvert\varepsilon_{t\max}\rvert < 4{,}500$
Maximum compression strain	$\lvert\varepsilon_{c\max}\rvert < 4{,}500$
Maximum shear strain	$\lvert\varepsilon_{xy\max}\rvert < 4{,}000$
Maximum torsion angle	$\theta_{\max} < 2.0°$
Maximum elastic axis flexivity	$U_{\max} < 1.3$ m
Stability	$\lambda_{\min} > 1.0$

Figure 2 Regions divided in the composite wing

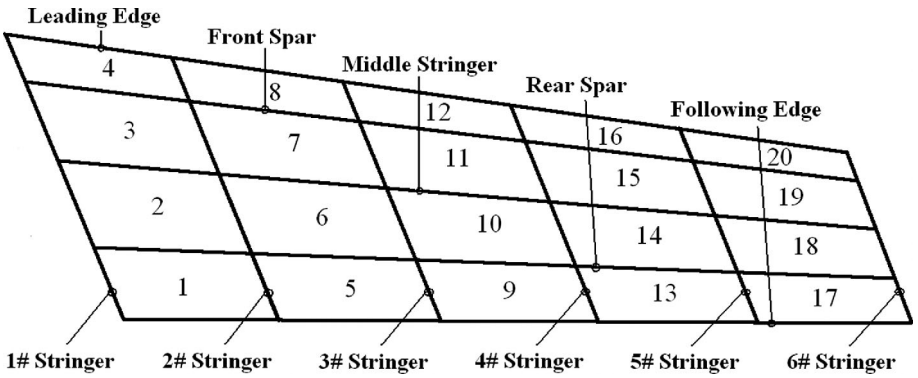

Figure 3 Optimization process

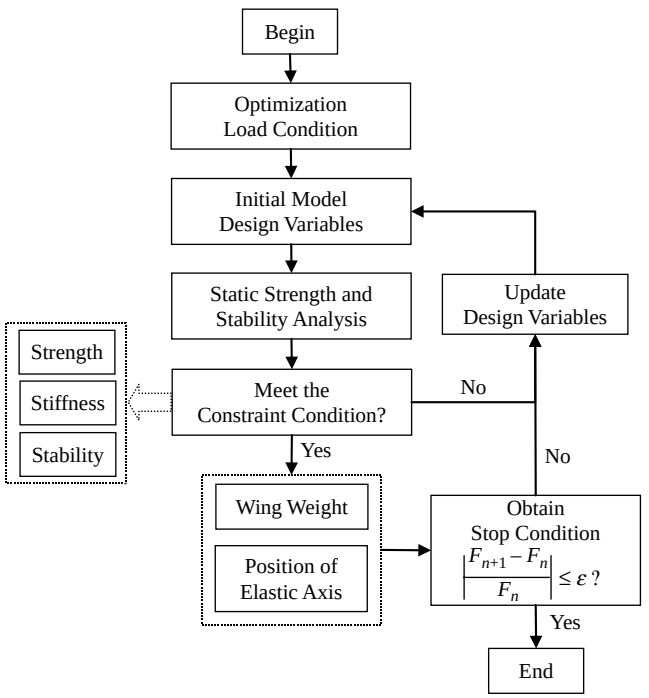

$$\left|\frac{F_{n+1}-F_n}{F_n}\right| \le \varepsilon \tag{19}$$

Where F_n is the optimum objective value at the n time iteration, ε is used to judge the convergence of the iteration and $\varepsilon = 1 \times 10^{-6}$ in the current optimization.

Optimization result

Table V shows optimization results under different weight coefficients. From Table V, it can be seen that both wing weight and *e/l* after optimization decrease under different weight coefficients, whereas divergent velocity increases. Comparing results under different weight coefficient values, it can be seen that weight coefficient has a direct impact on optimization results. It needs to be selected based on practical engineering problem. One-step of the optimization just includes static strength and stability analyzes using the FEM software NASTRAN and the elastic axis computation using a FORTRAN code, it costs about ten minutes, which is much faster than the traditional wing aeroelasticity optimization design method.

Table V Optimization results under different weight coefficients

	Wing weight		*e/l*		Divergent velocity	
Optimization results	Trend	Value (%)	Trend	Value (%)	Trend	Value (%)
$W_1 = 0.4$, $W_2 = 0.6$	Down	20.38	Down	10.86	Up	5.92
$W_1 = 0.5$, $W_2 = 0.5$	Down	21.57	Down	9.74	Up	5.26
$W_1 = 0.6$, $W_2 = 0.4$	Down	23.21	Down	9.23	Up	4.96

Table VI shows the optimization results of one cross section. It can be seen from Table VI that all of design parameters under different weight coefficient decrease, but they have their own scale under each weight coefficient. Comparing the results of the top skin with those of the down skin, it can be seen that the thickness of top skin is generally larger than that of the down skin. It is because that compression load is mainly applied on top skin, and a larger thickness value can avoid buckling. Moreover, it can be seen that the thickness of leading spar web is larger than that of the trailing spar web. It is because that the weight increase of the leading edge is conducive to the forward moving of the elastic axis.

We conclude that wing weight decreases and divergent velocity increases through aeroelasticity optimization design method based on elastic axis. Meanwhile, it can achieve an expected result but costs much less computational time than the conventional method. Computational efficiency is always the major concern in aircraft design. The aeroelasticity optimization design method based on elastic axis can be well used to solve the problem, especially for some large-scale structures.

Conclusions

The composite wing elastic axis is analyzed and an aeroelasticity optimization design method based on the elastic axis is put forward in the present work. Some useful conclusions can be drawn as follows:

- The wing cross-section was simplified to a thin walled structure with a single cell closed section and the composite material was converted into a 3D anisotropic material based on the material stiffness matrix with respect to the elastic axis.
- The location of the wing elastic axis has a direct impact on the divergent velocity. A wing elastic axis closer to the leading edge by changing the wing layout is preferred in wing design.

Table VI Optimization results of one cross section

Design parameter	Initial model	$W_1 = 0.4$, $W_2 = 0.6$	$W_1 = 0.5$, $W_2 = 0.5$	$W_1 = 0.6$, $W_2 = 0.4$
Top skin thickness/mm	4	3.8	3.5	3.1
Down skin thickness/mm	4	2.4	2.6	2.9
Leading spar web thickness/mm	5	4.0	4.0	3.9
Trailing spar web thickness/mm	5	2.7	3.0	3.1
Top stringer area/mm^2	624	602	595	592
Down stringer area/mm^2	624	493	497	463

- After aeroelasticity optimization design, the wing weight is decreased while the divergent velocity is increased. Meanwhile, it costs much less computational time than the conventional methods and can achieve an expected result.
- All of the design parameters under different weight coefficients decrease through aeroelasticity optimization design. In the optimization results, the thickness of the top skin is larger than that of the down skin while the thickness of the leading spar web is larger than that of the trailing spar web.

References

Alonso, J.J., LeGresley, P. and Pereyra, V. (2009), "Aircraft design optimization", *Mathematics and Computers in Simulation*, Vol. 79 No. 6, pp. 1948-58.

Barcelos, M. and Maute, K. (2008), "Aeroelastic design optimization for laminar and turbulent flows", *Computer Methods in Applied Mechanics and Engineering*, Vol. 197, pp. 1813-32.

Chintapalli, S., Elsayed, M.S.A., Sedaghati, R. and Abdo, M. (2010), "The development of a preliminary structural design optimization method of an aircraft wing-box skin-stringer panels", *Aerospace Science and Technology*, Vol. 14, pp. 188-98.

Dong, Y.P. and Wang, P.Y. *et al.* (2010), "Optimization analysis of the composite stiffness based on beam elements", *Journal of Materials Science & Engineering*, Vol. 28 No. 6, pp. 857-61.

Guo, S., Banerjee, J.R. and Cheung, C.W. (2003), "The effect of laminate lay-up on the flutter speed of composite wings", *Proceedings of the Institution of Mechanical Engineers, Part G (Journal of Aerospace Engineering)*, Vol. 217 No. 3, pp. 115-22.

Guruswamy, G.P. and Obayashi, S. (2004), "Study on the use of high-fidelity methods in aeroelastic optimization", *Journal of Aircraft*, Vol. 41 No. 3, pp. 616-19.

Jeon, K.S., Lee, J.W. and Byun, Y.H. (2008), "Multidisciplinary design approach using repetitive response surface enhancement and global optimization", *Proceedings of the 2008 Ninth ACIS International Conference on Software Engineering, Artificial Intelligence, Networking and Parallel/Distributed*, pp. 25-8.

Kameyama, M. and Fukunaga, H. (2007), "Optimum design of composite plate wings for aeroelastic characteristics using lamination parameters", *Computers and Structures*, Vol. 85, pp. 213-24.

Librescu, L. and Maalawi, K.Y. (2009), "Aeroelastic design optimization of thin-walled subsonic wings against divergence", *Thin-Walled Structures*, Vol. 47, pp. 89-97.

Liu, C.Y., Huang, G.N. and Wang, L.J. (2006), "Computation of stiffness characteristic of a high aspect ratio wing", *Airplane Engineer*, Vol. 4, pp. 21-4.

Mastroddi, F., Tozzi, M. and Capanolo, V. (2011), "On the use of geometry design variables in the MDO analysis of wing structures with aeroelastic constraints on stability and response", *Aerospace Science and Technology*, Vol. 15, pp. 196-206.

Palacios, R. and Cesnik, C.E.S. (2005), "Static nonlinear aeroelasticity of flexible slender wing in compressible flow", AIAA-2005-1945.

Riche, R.G.L. and Haftka, R.T. (1993), "Optimization of laminate stacking sequence for buckling load maximization by genetic algorithm", *AIAA*, Vol. 31 No. 5, pp. 951-6.

Venter, G. and Sobieszczanski-Sobieski, J. (2004), "Multidisciplinary optimization of a transport aircraft wing using particle swarm optimization", *Structural and Multidisciplinary Optimization*, Vol. 26 No. 11, pp. 121-31.

Wakayama, S. (2000), "Blended-wing-body optimization problem setup", AIAA Paper 2000-4740.

Yang, Q., Liang, Q. and Yang, Y.N. (2005), "Static aeroelastic optimization with CFD method", *Acta Aerodynamica Sinica*, Vol. 23 No. 1, pp. 16-20.

Zhang, K.S., Han, Z.H., Li, W.J. and Song, W.P. (2008), "Coupled aerodynamic/structural optimization of a subsonic transport wing using a surrogate model", *Journal of Aircraft*, Vol. 45 No. 6, pp. 2167-70.

Corresponding author

S.H. Huo can be contacted at: hshxin1985@163.com